

Integrated Simulations for Fast Ignition Targets

JOHZAKI Tomoyuki, NAGATOMO Hideo, MIMA Kunioki,
SAKAGAMI Hitoshi¹ and NAKAO Yasuyuki²

Institute of Laser Engineering, Osaka University, Suita 565-0871, Japan

¹*Department of Computer Engineering, University of Hyogo, Himeji 671-2201, Japan*

²*Department of Applied Quantum Physics and Nuclear Engineering, Kyushu University, Fukuoka 812-8581, Japan*

(Received: 9 December 2003 / Accepted: 20 March 2004)

Abstract

The basic issues of fast ignition scheme are radiation-hydrodynamics from implosion to fusion burning, relativistic laser-plasma interactions and core heating by fast electrons. For investigating the physics phenomena of fast ignition, “Fast Ignition Integrated Interconnecting code project” (FI³ project) has been proposed, where the each phenomenon is simulated with individual code and each code is collaborating with the others through the data transfer via the computer network. In the first step of the FI³ project, we carried out the integrated simulations for a cone-guided target and examined the implosion dynamics, the fast electron generation, and the core heating.

Keywords:

fast ignition, FI³ project, ALE hydro code, collective PIC code, relativistic Fokker-Planck code, cone-guided target

1. Introduction

In Fast Ignition (FI) scheme [1], an ultra-intense short-pulse laser is focused on pre-compressed plasma to heat it up to ignition temperature. Compared with the standard central hot-spark ignition scheme, the FI scheme would mitigate the requirement on uniformity of implosion and could obtain a high gain with a small-driver energy. Recent integrated experiments [2,3] for cone-guided targets demonstrated efficient fast heating of imploded cores.

For understanding the physics phenomena and proving fusion burning in the FI scheme, overall calculation, which includes the implosion dynamics, generation of fast electrons in relativistic laser-plasma interactions, core heating, and fusion burning processes, is indispensable. Each of physics phenomena, however, has different time and space scales and complicatedly interacts one another, so that it is practically impossible to simulate all phenomena with one code. In ILE (Institute of Laser Engineering), Osaka University and the related group, hence, “Fast Ignition Integrated Interconnecting code project” (FI³ project) [4] has been started, where the each phenomenon is simulated with individual code and the each code is collaborating with the others through the data transfer via the computer network.

In the first step of the FI³ project, we carried out integrated simulations, where each of processes is separately simulated, and the obtained results are transferred to the other codes. First, the ALE (Arbitrary Lagrangian Eulerian) radiation-hydro code [5] simulates the implosion process to

evaluate the core plasma profile at the maximum compression. Using this profile, the collective PIC (particle in cell) code [6] evaluates the time-dependent energy distribution of fast electron generated by the relativistic laser-plasma interactions. Finally, on the basis of a coupled Eulerian hydrodynamics and the RFP (Relativistic Fokker-Planck) code, the core heating process are simulated using both profiles (imploded core plasma and fast electron).

In the present paper, we will demonstrate the first results of overall FI simulations and discuss the implosion dynamics of a cone-guided target, time-dependent fast electron energy distribution, and core heating profiles.

2. Implosion dynamics of cone-guided targets

In FI scheme, a cone-guided target has been proposed to keep the propagation path of ignition laser free from the coronal plasma. We carried out 2-D (two dimensional) implosion simulations to study the implosion dynamics of such a none-spherical shell target. For the conventional multi-dimensional integrated implosion code, where Lagrangian-based ALE (Arbitrary Lagrangian Eulerian) methods are commonly used, it is very difficult to treat this kind of simulation because of the complex geometry which requires a sophisticated rezoning / remapping method and many times of trial and error during the execution. Therefore, we have extended CIP method [7] into ALE-CIP code “PINOCO” [5],

Corresponding author's e-mail: tjohzaki@ile.osaka-u.ac.jp

which enables to simulate the problem without any rezoning/remapping difficulty.

In the 2-D implosion code “PINOCO”, two temperature plasma, Spitzer-Harm type thermal transport, radiation transport, LTE (local thermodynamic equilibrium) and CRE (collisional radiative equilibrium) opacity and emissivity, equation of state, laser ray-trace, laser absorption are considered. For the thermal diffusion equations and multi-group diffusion type radiation transport equation, the implicit 9-point difference equations are solved by ILUBCG method. For the laser ray-trace, a simple 1-D (one-dimensional) ray-tracing method is applied.

A target shell of polystyrene ($\rho = 1.06 \text{ g/cm}^3$) has a uniform thickness of $8 \text{ }\mu\text{m}$ and an inner radius of $250 \text{ }\mu\text{m}$. The cone with an opening angle of 30 degree is attached to the shell. The similar experiment was performed at GXII laser facility of ILE to demonstrate the FI [2,3]. The target is uniformly irradiated by 6 kJ (on target) Gaussian-pulse-shaped green laser ($\lambda = 0.53 \text{ }\mu\text{m}$). In these simulations, we have ignored the radiation transport for the limitation of the CPU time.

In **Fig. 1**, Density contours at 1.93 ns when the maximum average ρR was measured is shown. Although the edge of the shell was delayed under the influence of the conical target, the shell target was compressed to more than 200 g/cc at the maximum. Because of the pressure imbalance due to the existence of Au-cone, the hot spot was moved to the left-hand side. In the spherical implosion, the shell target was rebound by the hot spot located at the center after the maximum compression at 1.90 ns [**Fig. 2**]. In non-spherical case, however, the shell continued to be imploded due to the loss of hot spot at the moment, and then the dense main fuel part is concentrated at the center. As the result, the average ρR of the cone-guided target reached the maximum at 1.93 ns, and the value becomes twice larger than that of the spherical case.

3. Relativistic laser-plasma interactions

For evaluation of fast electron generation due to relativistic laser-plasma interactions, we use the 1-D collective PIC code [6], where collective particles are used to represent many normal particles and then total number of particles and computations are drastically reduced. The density profile in the inner side of Au-cone at the maximum compression was obtained from ALE hydro code and was introduced as an initial plasma into the PIC system. The Gaussian pulse of wavelength $\lambda_L = 1.06 \text{ }\mu\text{m}$ and FWHM (full width at half maximum) = 300 [fs] was assumed as the ignition laser. We carried out the collective PIC simulations for the laser intensity of $I_L = 10^{19}$ and $10^{20} \text{ [W/cm}^2]$ and evaluated time-dependent energy spectrum and intensity of forward-directed fast electrons every 20 [fs] at $100 n_{cr}$ point.

The temporal evolution of fast electron intensities are plotted in **Figure 3**. In both cases ($I_L = 10^{19}$ and $10^{20} \text{ [W/cm}^2]$), the electron beam pulse length is almost the same as the laser pulse length. The energy transfer rates from the

laser to the forward directed fast electrons ($E_{fe} > 50 \text{ keV}$) are 19% and 21% for the case of $I_L = 10^{19}$ and $10^{20} \text{ [W/cm}^2]$, respectively. The energy spectrum of fast electrons passing through the $100 n_{cr}$ point per unit time at every 100 [fs] from

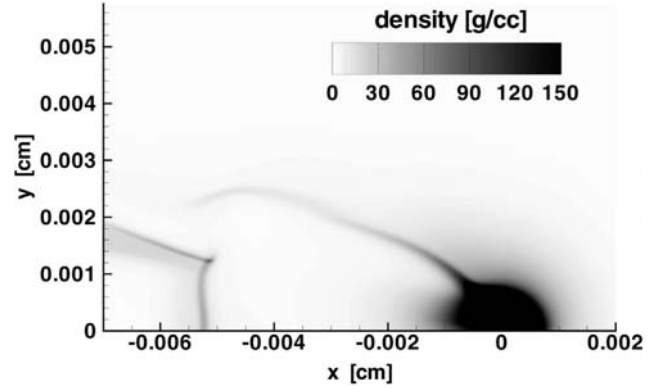


Fig. 1 Mass density (g/cc) contours at $t = 1.93 \text{ ns}$ when the maximum average ρR is measured.

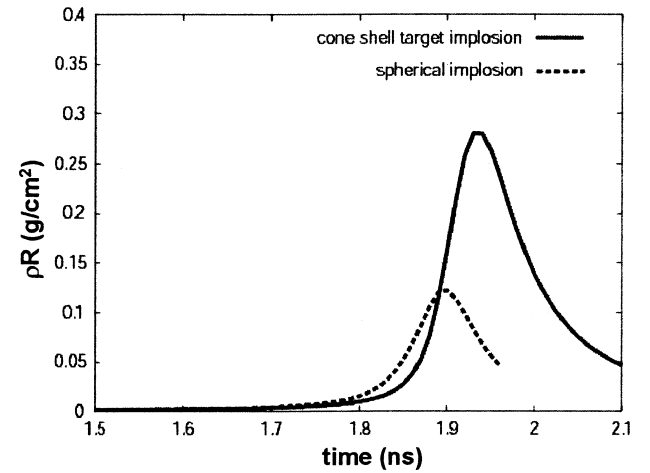


Fig. 2 Time history of average ρR . Solid line indicates the simulated result of non-spherical implosion with cone target, and dotted line indicates the spherical implosion case.

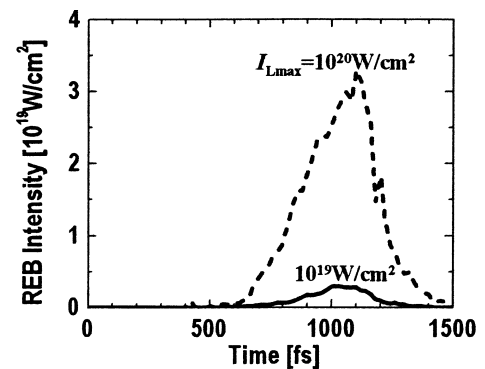


Fig. 3 Temporal profiles of intensity of forward-directed fast electrons.

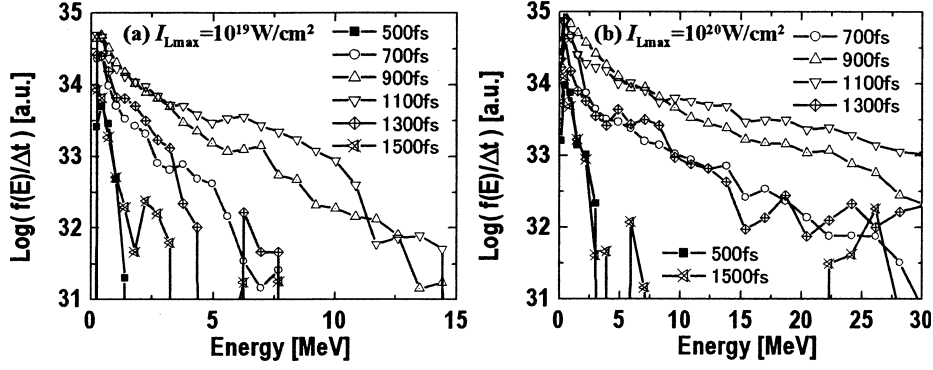


Fig. 4 Momentarily energy spectrum of forward-directed fast electrons passing through the $100 n_{cr}$ point per unit time at every 100 [fs] from $t = 500$ to 1,500 [fs].

$t = 500$ to 1500 [fs] are plotted (a) for $I_L = 10^{19}$ [W/cm²] and (b) for $I_L = 10^{20}$ [W/cm²] in Fig. 4. (In this and the next sections, the time t was set to be 0 at the beginning of ignition laser.) The average energy of fast electrons estimated from time-integrated spectrum are 1.7 and 5.3 [MeV] for $I_L = 10^{19}$ and 10^{20} [W/cm²]. It is found, however, that the momentarily energy spectrum changes with time. At the beginning of the electron beam pulse, the energy of generated electrons is relatively low ($E_{fe} < a \text{ few [MeV]}$). At $t = 500$ [fs], the average energies of fast electrons \bar{E}_{fe} are 0.5 and 1.0 [MeV] for the cases of $I_L = 10^{19}$ and 10^{20} [W/cm²], respectively. The high-energy component gradually increases with time. At the time when the intensity of electron beam pulse becomes the maximum ($t \sim 1100$ [fs]), the average energy of fast electrons also becomes the maximum ($\bar{E}_{fe} = 2.6$ [MeV] for $I_L = 10^{19}$ [W/cm²] and 8.8 [MeV] for $I_L = 10^{20}$ [W/cm²]). After that, the high-energy component decreases with time, and then becomes 0.6 [MeV] for $I_L = 10^{19}$ [W/cm²] and 2.3 [MeV] for $I_L = 10^{20}$ [W/cm²] at $t = 1500$ [fs].

For core heating analysis, not the time integrated, but the time-dependent energy spectrum of fast electrons is important.

4. Imploded core heating by fast electrons

A 1-D RFP code [8] has been developed for analysis of the fast electron transport and energy deposition processes in dense core plasma. Recently, this code was extended to 2-D one and coupled with a Eulerian hydro code to examine core-heating properties. In this code, cold bulk electrons and ions are treated by a 1-fluid and 2-temperature hydro model, and the fast electrons generated by the ignition laser-plasma interactions are treated by the RFP model. In the coupled RFP-hydro code includes magnetic field generated by fast electron current, gradient of plasma resistivity and pressure gradient.

Using the RFP-hydro code, we examined the core heating properties in a cone-guided target. As an imploded-core profiles, we use results of the ALE radiation-hydro simulation (shown in Sec. 2). The time-dependent momentum distribution of fast electrons evaluated by the 1-D collective PIC code (shown in Sec. 3) was used as the fast electron

sources. The fast electrons were injected at the inner side of Au-cone by assuming the Gaussian profile of FWHM = 15 μm in the perpendicular direction. The simulations were also carried out for mono-energy electron beams ($E_0 = 1, 2$ and 5 MeV) with Gaussian profile ($\tau_{FWHM} = 300$ [fs]). The peak intensity of these electron beams was assumed almost the same value as that obtained in the PIC simulations for $I_L = 10^{20}$ W/cm², *i.e.* $I_{REB} = 3 \times 10^{19}$ W/cm².

Figure 5 shows the contours of the heating rate by fast electrons when the heating rate in the dense core becomes the maximum ($t = 800$ fs). (The density contours are also plotted by lines.) It is found from this figure that the fast electrons injected at the inner side of the cone propagate into the dense core and they deposit some fraction of their kinetic energy there due to the Coulomb interactions.

In Fig. 6, the temporal profiles of (a) the heating rate and (b) the ion temperature averaged over the dense core region are plotted as a function of time for five different electron beam conditions, *i.e.* PIC sources of $I_L = 10^{19}$ and 10^{20} [W/cm²], mono-energy sources of $E_0 = 1, 2$ and 5 [MeV] with peak intensity of 3×10^{19} [W/cm²]. The energy deposition rate per unit path length of a fast electron decreases with the electron energy. In addition, the number of injected fast electrons decreases with the beam electron energy under the fixed beam intensity. Thus, in the 1-MeV mono-energy beam

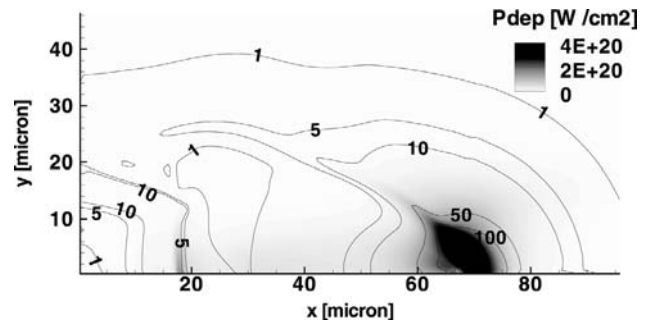


Fig. 5 Contours of heating rate by fast electrons, ρ_{dep} [W/cm²] (black and white) and core density [g/cc] (lines) when the core heating rate becomes the maximum ($t = 800$ fs) in the case of $I_L = 10^{20}$ [W/cm²].

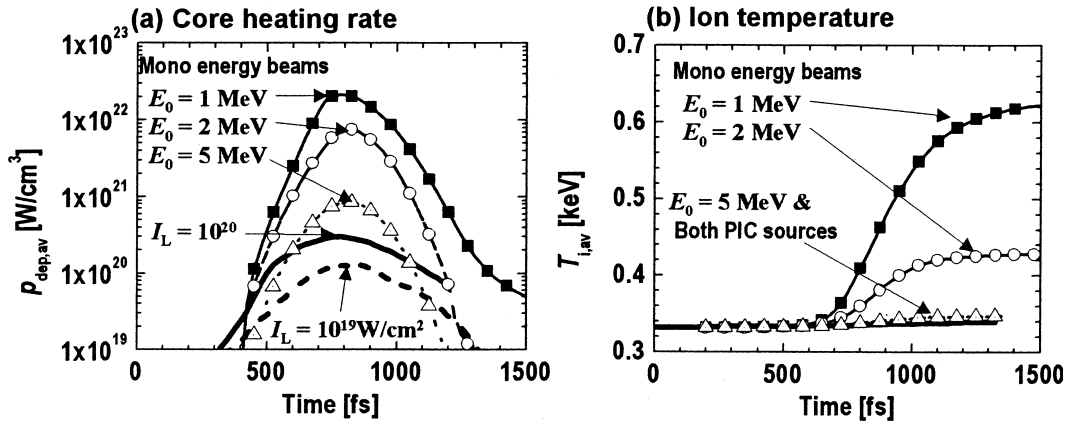


Fig. 6 Temporal profiles of (a) Core heating rate, $p_{dep,av}$ and (b) ion temperature, $T_{i,av}$ averaged over the core region ($\rho > 50$ g/cc).

case, the core heating rate is the largest among three mono-energy beam cases, and then the core temperature becomes the highest. The electron beam obtained from PIC simulation for $I_L = 10^{20}$ [W/cm²] has almost the same intensity as the mono-energy beams. The average energy of electrons, however, is excessively high ($\bar{E}_{fe} = 8.8$ [MeV] at the peak intensity, 5.5 [MeV] for the time-integrated spectrum), so that the range is too long. On the other hand, in the case of PIC source of $I_L = 10^{19}$ [W/cm²], the average energy is relatively low, but the intensity is also low. Thus, the core heating rate obtained in both PIC source cases is too small to raise the bulk plasma temperature.

5. Summary

In the first stage of FI³ project, we demonstrated the integrated simulations for a cone-guided target and examined the implosion dynamics, the fast electron generation, and the core heating. The implosion simulations using CIP-based ALE code showed that the areal density of cone-guided target becomes twice larger than that of the spherical target because of loss of central hot spot. The time-dependent fast electron momentum distribution was estimated by the 1-D collective PIC simulations, in which the density profile of inner side of Au-cone obtained from implosion simulations was used. Finally, the core heating was simulated by the coupled RFP-hydro code where we used the imploded core profiles and the fast electron profiles obtained from the ALE hydro code and the collective PIC simulations, respectively. We could not obtain expected core heating in the present simulations,

since the energy of fast electrons was too high for $I_L = 10^{20}$ [W/cm²] and the intensity of fast electron beam was too low for $I_L = 10^{19}$ [W/cm²].

For more realistic estimations, each of the code is required the model improvement (*e.g.* consideration of magnetic field generation during implosion, multi-dimensional effect in the fast electron generation and recirculation of fast electrons due to the sheath field generated around the core. In near future, we will start “on-line” integrated simulations.

References

- [1] M. Tabak *et al.*, Phys. Plasmas, **1**, 5, 1626 (1994).
- [2] R. Kodama *et al.*, Nature, **412**, 798 (2001).
- [3] R. Kodama *et al.*, Nature, **418**, 933 (2002).
- [4] H. Sakagami *et al.*, Proc. of the 2nd Int. Conf. on Inertial Fusion Science and Applications, Kyoto 2001, IFSA 2001, Elsevier, 380 (2001).
- [5] H. Nagatomo *et al.*, Proc. of 2nd Int. Conf. on Inertial Fusion Sciences and Applications, Kyoto 2001, IFSA 2001, Elsevier, 140 (2001).
- [6] H. Sakagami *et al.*, Proc. of 3rd Int. Conf. On Inertial Confinement Fusion Science and Applications, Monterey, CA 2003, IFSA2003, American Nuclear Society, 434 (2004).
- [7] T. Yabe *et al.*, J. Comput. Phys. **169**, 556 (2001).
- [8] T. Johzaki *et al.*, Fusion Sci. Technol. **43**, 3, 428 (2003).